

# Micropolar Fluid Flow Through a Porous Stretching/Shrinking Sheet with Mass Transpiration: An Analytical Approach

RISHU GARG<sup>1,3</sup>, JITENDER SINGH<sup>1,3</sup>, U. S. MAHABALESHWAR<sup>2,3</sup>,  
OKHUNJON SAYFIDINOV<sup>3</sup>, G. BOGNAR<sup>3\*</sup>

<sup>1</sup>Department of Mathematics,  
Guru Nanak Dev University,  
Amritsar, Punjab, 143005,  
INDIA

<sup>2</sup>Department of Studies in Mathematics,  
Davangere University,  
Shivagangothri, Davangere, 577 007,  
INDIA

<sup>3</sup>Institute of Machine and Product Design,  
Faculty of Mechanical Engineering and Informatics,  
University of Miskolc,  
Miskolc-Egyetemváros, H-3515 Miskolc,  
HUNGARY

*\*Corresponding Author*

**Abstract:** - In this paper, the flow of a micropolar fluid over a stretching or shrinking sheet is investigated under magnetohydrodynamic (MHD) conditions. Such a flow is described by highly nonlinear PDEs. Using the similarity transformation technique, the PDEs governing the flow are reduced to a system of nonlinear ODEs, which further allows a closed-form analytical solution. The effect of the microrotation on the skin friction coefficient, the dimensionless forms of the velocity, and the temperature flow fields in the neighborhood of the stretching or shrinking sheet are discussed for various combinations of the dimensionless parameters. The numerical results reveal that the micropolar flow may accelerate or decelerate depending upon the numerical values of the mass transpiration and the permeability of the porous sheet. An increase in the tangential and the angular flow velocities is found to occur with an increase in the microrotation. Further, it is observed that the increase in the microrotation increases the skin friction coefficient.

**Key-Words:** - Micropolar fluid, porous medium, magnetohydrodynamics (MHD), dual solutions, stretching sheet, shrinking sheet

Received: October 11, 2022. Revised: May 14, 2023. Accepted: June 15, 2022. Published: July 18, 2023.

## 1 Introduction

Dynamics of boundary layer flow due to stretching or shrinking sheets has been the subject of active research for decades since these boundary layer flows have witnessed practical applications such as in the drawing of plastic sheets, films, wires, entropy generation, etc., [1]. The stretching sheet problem was first discussed by, [2], [3]. In, [4], the author extended recent work for Newtonian fluids varying from the slit. Inspired by this research, many investigations have been done concerning the flow and heat transfer problems under various

physical conditions. In, [5], the authors have analyzed the combined effect of the heat source or heat sink parameter and the stress for both viscous as well as inviscid fluids along with the MHD conditions and chemical reaction parameters. In the presence of a porous medium, analytical solutions for the boundary layer flow for a variety of boundary conditions have been obtained by, [6]. In, [7], the authors discussed mass transpiration in nonlinear MHD boundary layer flow due to a porous stretching sheet. In, [8], the author investigated heat transfer enhancing features with the non-Fourier

Cattaneo Christov model. In, [9], the author investigated the electro-osmotic flow of a third-grade fluid in a micro-channel in the presence of MHD. In, [10], the authors investigated the Cattaneo-Christov double diffusion and radiative heat flux in the bio-convective flow of Maxwell liquid. In, [11], [12], the authors investigated the stretching sheet problems for nanofluid boundary layer flows. In, [13], the authors analyzed the chemically reactive aspects of the flow of tangent hyperbolic material. Later, in the study, [14], the authors investigated the flow of a second-grade nanofluid in view of optimizing entropy generation.

A micropolar fluid is a fluid with microstructure. Such fluids belong to the class of fluids having asymmetric stress tensors. In this paper, we shall call them polar fluids. So, polar fluids include as a special case, the well-known classical fluids. In practice, a micropolar fluid is a suspension of rigid, randomly oriented (or spherical) particles in a viscous carrier, where the deformation of the suspended particles is assumed to be negligible.

The present research focuses on the flow problems related to viscous as well as inviscid fluids. Some researchers have shown interest to analyze stretching sheet problems in micropolar fluids. In, [15], the author is credited to have initiated the theoretical model of micro fluids. Eringen's theory of micropolar fluids played a central role in the early analysis of the practical features of numerous complex flows. Micropolar fluids are a type of microfluid, and that has been studied by, [16]. Further, [17], [18], have analyzed several flow problems considering micropolar fluids.

In the flow equation, micropolar fluids have both a vector of classical velocity as well as a vector of microrotation. The mass and momentum connection illustrates the effect of the couple stress, the spin-inertia, and the microrotation on some characteristics of the fluid under consideration, [19], [20]. Several researchers have investigated the flow of micropolar fluids in the presence of MHD and porous medium. In, [21], the authors investigated the flow of a micropolar fluid due to a stretching sheet while taking into account the impact of the temperature-dependent viscosity and the variable surface temperature. Micropolar fluids and heat transmission caused by porous shrinking sheets have been studied, [22]. In, [23], the author used an analytical approach to study the effect of a micropolar fluid over a linear stretching sheet.

The micropolar fluid model as introduced by Eringen elegantly describes the dynamics of such fluids. Eringen's model is a generalization of the existing Navier-Stokes model and has a much wider

range of applicability than the classical one, both in theory as well as in practice. Further, the micropolar fluid model is simple to apply, which makes it interesting and suitable for use by researchers.

Finding closed-form solutions for boundary layer flows regarding stretching or shrinking sheet problems is another challenge. In view of this, in, [24], [25], [26], the authors have obtained analytical solutions for some of the related flow problems. The most popular technique in dealing with closed-form solutions of the boundary layer equations is to apply the similarity transformations. The present work is motivated by the earlier research, [27], [28], and it focuses on investigating micropolar fluid flow due to stretching, or shrinking sheet under mass transpiration. Using the well-known method of similarity transformations, the PDEs governing the underlying boundary layer flow are transformed into a system of ODEs, which along with the appropriate boundary conditions lead to a two-point boundary value problem in ODEs. The resulting boundary value problem is solved analytically to obtain closed-form solutions. The closed-form solution can be unique, or exhibit dual behavior. The dual behavior is expected for the case of the shrinking sheet, which is also investigated numerically. The present and stated fluid, micropolar fluid flow, has several applications, particularly in the study of rheological complex fluids, such as colloidal fluids, polymeric suspension, liquid crystals, animal blood, etc. Micropolar fluid flows have practical applications in lubrication and flow through porous media.

## 2 Nomenclature

Variable	Description	SI Units
$a$	Constant	$(s^{-1})$
$C$	Permeability of porous medium	$(m^3 s^{-1})$
$N$	Microrotation	$(s^{-1})$
$j$	Microrotation per unit mass	$(kg^{-1} s^{-1})$
$S$	Suction/injection parameter	$(-)$
$K$	Microrotation parameter	$(-)$
$f$	Dimensionless transverse velocity	$(-)$
$f_\eta$	Dimensionless Tangential velocity	$(-)$
$(u, v)$	Flow velocity in Cartesian	$(ms^{-1}, ms^{-1})$

	coordinates	
$v_w$	Stefan blowing velocity	$(ms^{-1})$
$\alpha$	Stretching/shrinking parameter	$(-)$
$\beta$	Solution domain	$(-)$
$\Lambda$	Porous medium parameter	$(-)$
$m$	Vortex viscosity	$(m^3s^{-2})$
$\nu$	Kinematic viscosity	$(m^2s^{-1})$
$\gamma^*$	Spin gradient viscosity	$(ms)$
$\rho$	Fluid density	$(kg\ m^{-3})$
$w$	Wall condition	$(-)$
B.Cs	Boundary conditions	$(-)$
MHD	Magnetohydrodynamics	$(-)$
ODEs	Ordinary differential equations	$(-)$
PDEs	Partial differential equations	$(-)$

### 3 Problem Formulation

We consider a steady, incompressible two-dimensional boundary layer flow of a micropolar fluid through a porous medium. The Cartesian coordinates  $x$  and  $y$  are taken along the surface and are normal to it with  $u$  and  $v$  as respective velocity components. The governing boundary layer equations are

$$\frac{\partial u}{\partial x} + \frac{\partial v}{\partial y} = 0, \quad (1)$$

$$u \frac{\partial u}{\partial x} + v \frac{\partial u}{\partial y} = \left( \nu + \frac{m}{\rho} \right) \frac{\partial^2 u}{\partial y^2} + \frac{m}{\rho} \frac{\partial N}{\partial y} - \frac{\mu}{\rho c} u, \quad (2)$$

$$u \frac{\partial N}{\partial x} + v \frac{\partial N}{\partial y} = \frac{\gamma^*}{\rho j} \frac{\partial^2 N}{\partial y^2} - \frac{m}{\rho j} \left( 2N + \frac{\partial u}{\partial y} \right), \quad (3)$$

where  $\rho$  is the fluid density,  $\nu$  is the kinematic viscosity,  $N$  is the microrotation or angular velocity,  $j = (\nu/c)$  is the microinertia per unit mass,  $\gamma^* = (\mu + m/2)j$  and  $m$  are the spin gradient viscosity and the vortex viscosity, respectively.

#### 3.1 Boundary Conditions

The boundary conditions for the proposed model are the following:

$$u = u_w(x) = cx, \quad v = v_w \text{ at } y = 0; \\ u \rightarrow 0 \text{ as } y \rightarrow \infty, \quad (4)$$

$$N = -n \frac{\partial u}{\partial y} \text{ at } y = 0; \\ N \rightarrow 0 \text{ as } y \rightarrow \infty, \quad (5)$$

where  $v_w$  is the surface mass transfer velocity with  $v_w < 0$  for the case of suction and  $v_w > 0$  for the case of injection. Here,  $N$  denotes the microrotation or angular velocity. The boundary parameter  $n$  in Eq. (5) satisfies  $0 \leq n \leq 1$ . Here  $n = 0$  corresponds to the situation when microelements at the stretching sheet are unable to rotate and denotes weak concentrations of the microelements at the sheet. The case  $n = 1/2$  corresponds to the vanishing of the anti-symmetric part of the stress tensor and it shows weak concentration of microelements. Finally, the case  $n = 1$  is for turbulent boundary layer flows.

#### 3.2 Similarity Transformations

In order to transform the governing PDEs into a system of non-linear ODEs, we introduce the following dimensionless and similarity variables for Eqs. (2) and (3):

$$\eta = (a/\nu)^{\frac{1}{2}} y, \quad u = axf'(\eta), \\ v = -(a\nu)^{\frac{1}{2}} f(\eta), \quad N = (a/\nu)^{\frac{1}{2}} axg(\eta), \quad (6)$$

where  $a$ , is constant. Using Eq. (6) in Eqs. (1)-(3), we get the following ODEs:

$$(1 + K)f'''' + ff'' - (f')^2 + Kg' - \Lambda^2 f' = 0, \quad (7)$$

$$\left( 1 + \frac{K}{2} \right) g'' + fg' - f'g - 2Kg - Kf'' = 0, \quad (8)$$

where the primes denote differentiation with respect to  $\eta$ ,  $K$  is the microrotation parameter, and  $\Lambda$  is the porous medium parameter. These parameters and dimensionless numbers are defined as follows:

$$K = \frac{m}{\mu}, \quad \Lambda = \frac{\mu}{\rho a c}. \quad (9)$$

The transformed boundary conditions (4)-(5) become

$$\eta = 0, \quad f(0) = S, \quad f'(0) = c/a = \alpha, \\ g(0) = -nf''(0), \quad (10)$$

$$\eta \rightarrow \infty, \quad f'(\eta) \rightarrow 0, \quad g(\eta) \rightarrow 0, \quad (11)$$

where  $S$  is the suction/injection parameter, and  $\alpha$  is the stretching/shrinking parameter.

The local skin friction coefficient is given by

$$C_{fx} = [(\mu + m) \frac{\partial u}{\partial y} + mN]_{y=0} / (\rho u_w^2). \quad (12)$$

In the dimensionless form, the local skin friction coefficient can be expressed as

$$Re_x^{1/2} C_{fx} = [1 + (1-n)K] f''(0), \quad (13)$$

where  $Re_x = ax^2/\nu$  denotes the local Reynolds number.

#### 4 Analytical Solution

For weak concentration, that is, for  $n = 1/2$ , Eqs. (7)-(8) along with boundary conditions (10)-(11) have the exact solution of the form

$$f(\eta) = S + \frac{\alpha}{\beta}(1 - e^{-\beta\eta}), \quad g(\eta) = \frac{\alpha\beta}{2} e^{-\beta\eta}, \quad (14)$$

Substituting Eq. (14) in Eq. (7), we get a quadratic equation for  $\beta$ :

$$(K + 2)\beta^2 - 2S\beta - 2(\alpha + \Lambda) = 0. \quad (15)$$

Solving Eq. (15) we get

$$\beta = \frac{1}{K+2} (S \pm \sqrt{S^2 + 4\Lambda + 4\alpha + 2K(\Lambda + \alpha)}). \quad (16)$$

Thus, the closed-form solutions of Eq. (7)-(8) subject to the boundary conditions (10) -(11) are given by

$$f(\eta) = S + \frac{\alpha(K + 2)}{S \pm \sqrt{S^2 + 4\Lambda + 4\alpha + 2K(\Lambda + \alpha)}} \times \left( 1 - \exp \left[ -\eta \frac{S \pm \sqrt{S^2 + 4\Lambda + 4\alpha + 2K(\Lambda + \alpha)}}{K+2} \right] \right), \quad (17)$$

$$g(\eta) = \frac{\alpha}{2} \frac{(S \pm \sqrt{S^2 + 4\Lambda + 4\alpha + 2K(\Lambda + \alpha)})}{K + 2} \times \left( \exp \left[ -\eta \frac{S \pm \sqrt{S^2 + 4\Lambda + 4\alpha + 2K(\Lambda + \alpha)}}{K+2} \right] \right). \quad (18)$$

The velocity profile is determined after differentiating Eq. (17) once, and we have

$$f'(\eta) = \alpha \exp \left[ -\eta \frac{S \pm \sqrt{S^2 + 4\Lambda + 4\alpha + 2K(\Lambda + \alpha)}}{K+2} \right]. \quad (19)$$

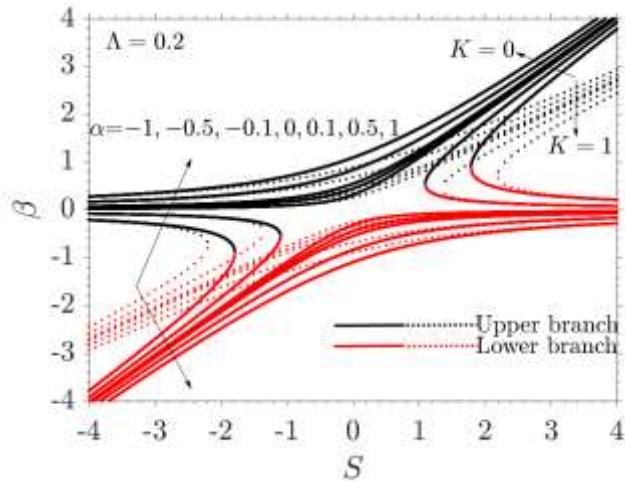
The skin friction coefficient in closed form is given by

$$Re_x^{1/2} C_{fx} = -(1 + K/2)\alpha\beta. \quad (20)$$

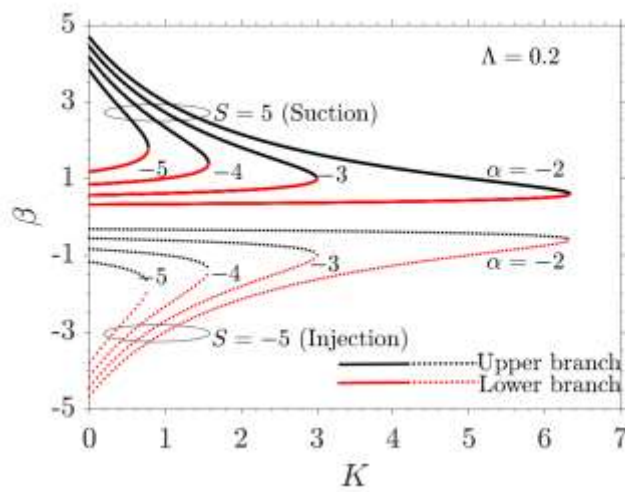
#### 5 Results and Discussion

Figure 1a shows the solution domain in the  $(S, \beta)$ -plane for a fixed parametric value of  $\Lambda=0.2$ . The solid and dotted lines in the Figure 1a correspond to  $K=0$ , and  $K=1$ , respectively. The black and red portions of the curves correspond to the upper and lower branches of the dual solution, wherein different curves have been drawn for seven different values of  $\alpha = -1, -0.5, -0.1, 0, 0.1, 0.5, 1$ . We observe that the upper branch of the solution domain shifts upwards in the  $(S, \beta)$ -plane by increasing the values of  $\alpha$ . We note that for  $\alpha = -1$ , the solution exists only for  $S < -2$ , or  $S > 2$ . For the other considered values of  $\alpha$ , the solution exists for all values of  $S$ . The effect of shifting the curves reverses in the case of the lower branch of the solution domain. Further, it is observed that the solution domain shifts downwards in the  $(S, \beta)$ -plane on varying microrotation parameter  $K$  from 0 to 1.

The behavior of the solution domain in the  $(K, \beta)$ -plane is shown in Figure 1b for  $\Lambda = 0.5$ . The solid and dotted lines in the Figure 1a correspond to  $S = 5$ , and  $S = -5$ , respectively. The black and red portions of the curves correspond to the upper and lower branches of the dual solution. The different curves have been drawn for four different values of  $\alpha = -5, -4, -3, -2$ . Here, the solution domain in the  $(K, \beta)$ -plane increases by increasing the values of stretching/shrinking parameter  $\alpha$  for the upper branch solution but the effect reverses in the case of the lower branch solution. Also, it is observed that the solution domain occurs for a larger value of  $\beta$  in the suction case as compared to the injection case.



(a)

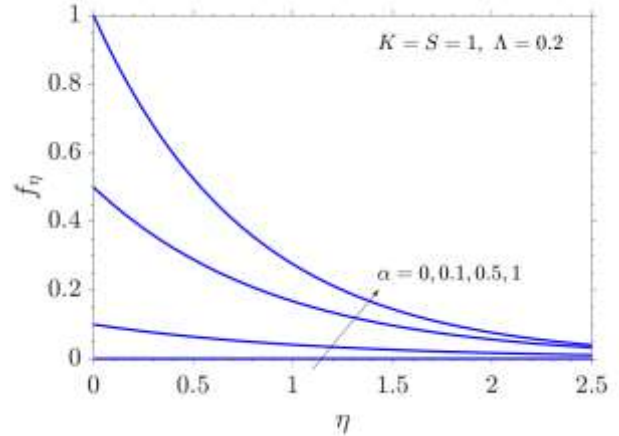


(b)

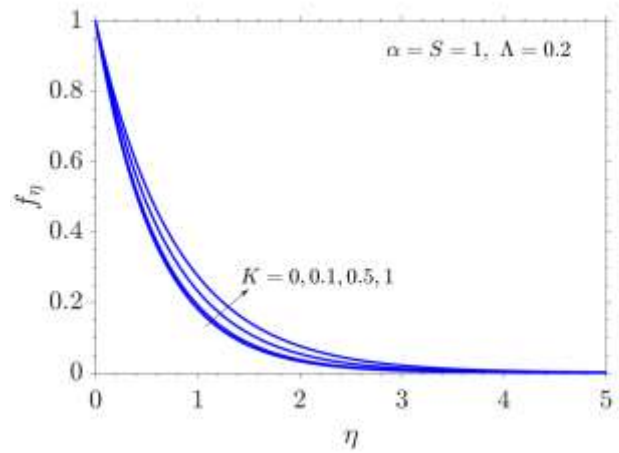
Fig. 1: The solution domain for  $\beta$  as a function of (a) mass transpiration  $S$  and (b) microrotation parameter  $K$ .

Figure 2a portrays the effect of various values of stretching/shrinking parameter  $\alpha = 0, 0.1, 0.5, 1$ ,  $K = S = 1$ ,  $\Lambda = 0.2$  on the tangential velocity component  $f_\eta(\eta)$ . From these graphs, we observe that the tangential velocity component  $f_\eta(\eta)$  increases with an increase in the value of  $\alpha$ . Apart from the usual behavior of a decrease in  $f_\eta(\eta)$  with  $\eta$ , we observe that the rate of decrease of  $f_\eta(\eta)$  with  $\eta$  increases sharply as the parameter  $\alpha$  is varied from 0 to 1.

Similar variations of the profile  $f_\eta(\eta)$  with  $\eta$  are found to occur on varying  $K$ , which have been depicted in Figure 2b for  $K = 0, 0.1, 0.5, 1$ ,  $\alpha = S = 1$ ,  $\Lambda = 0.2$ .



(a)



(b)

Fig. 2: The velocity profiles  $f_\eta(\eta)$  for various values of (a) stretching/shrinking parameter  $\alpha$  and (b) microrotation parameter  $K$ .

Figure 3a shows the effect of various values of  $\Lambda = 1, 2, 3, 4$ ,  $\alpha = S = 1$ ,  $K = 0.2$  on the profile of  $f_\eta(\eta)$ . Clearly the profile of  $f_\eta(\eta)$  shifts upwards on incrementing  $\Lambda$  from 1 to 4.

Similar variations in the profile of  $f_\eta(\eta)$  can be observed from Figure 3b when  $S$  is incremented from -1 to 1 for  $\alpha = \Lambda = 1$ ,  $K = 0.2$ .

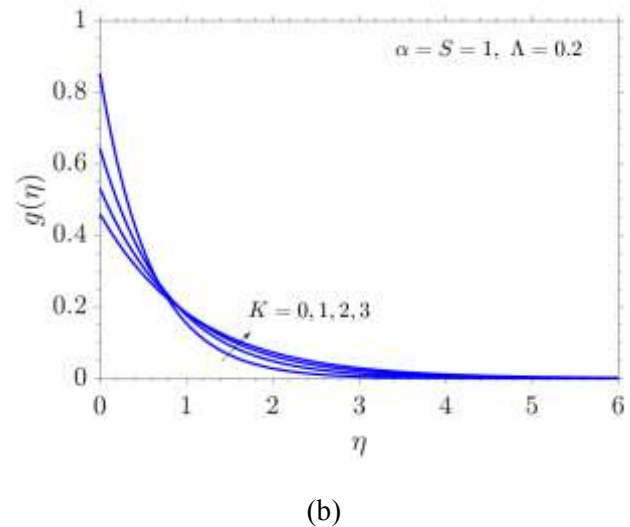
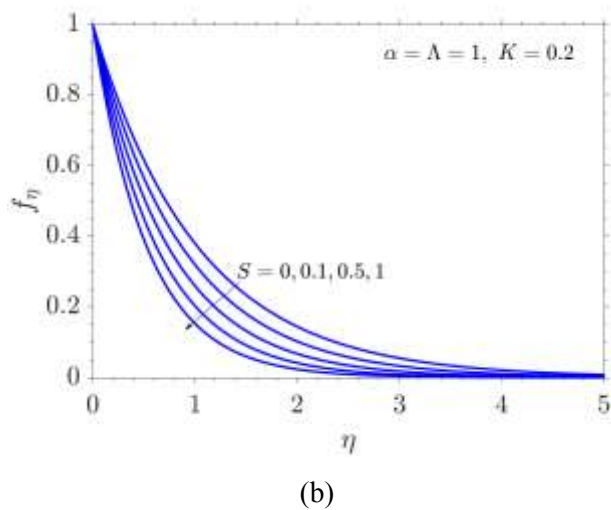
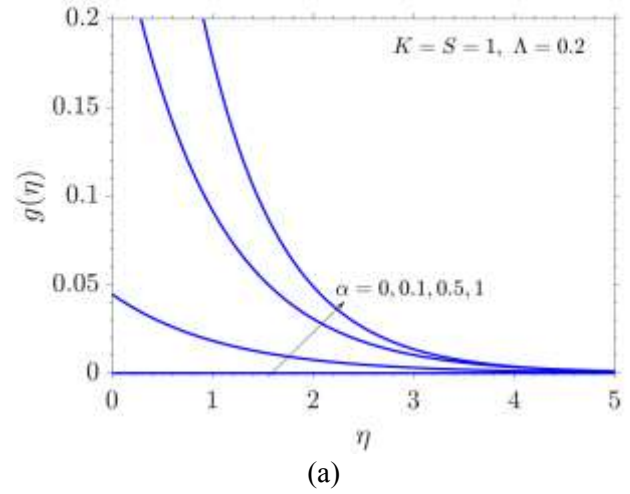
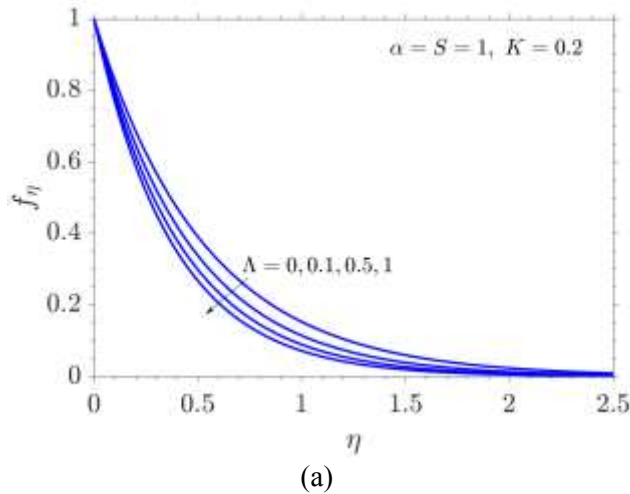


Fig. 3: The tangential velocity profiles  $f_{\eta}(\eta)$  for various values of (a) porous medium parameter  $\Lambda$  and (b) mass transpiration  $S$ .

Fig. 4: The angular velocity profiles  $g(\eta)$  for various values of (a) stretching/shrinking parameter  $\alpha$  and (b) microrotation parameter  $K$ .

Figure 4a shows the effect of various values of  $\alpha = 0, 0.1, 0.5, 1$ , on the profile of the angular velocity  $g(\eta)$  for fixed parametric values of  $K = S = 1$ , and  $\Lambda = 0.2$ . We find that  $g(\eta)$  is an increasing function of  $\alpha$ .

On the other hand, when the parameter  $K$  is incremented from 0 to 3, the variations in the profile of  $g(\eta)$  are dramatic, which can be observed from Figure 4b, for the fixed parametric values of  $\alpha = S = 1$ ,  $\Lambda = 0.2$ . Here,  $g(\eta)$  increases on incrementing  $K$  at any fixed location near the slit, while  $g(\eta)$  decreases with  $K$  at a location sufficiently away from the slit.

Figure 5a shows the effect of various values of  $\Lambda = 0, 1, 2, 3$ , on the profile of the microrotation  $g(\eta)$  for the fixed parametric values of  $\alpha = S = 1$ ,  $K = 0.2$ . Clearly  $g(\eta)$  increases with an increase in the values of  $\Lambda$  for small values of  $\eta$  and decreases with  $\Lambda$  for all sufficiently large  $\eta$ . So, microrotation is favored by the porosity of the medium near the slit while the microrotation is hindered by the porosity of the medium away from the slit.

A similar variation of the profile of  $g(\eta)$  by varying  $S$  which has been shown in Figure 5b for the fixed parametric values of  $\alpha = 1$ ,  $K = \Lambda = 0.2$ .

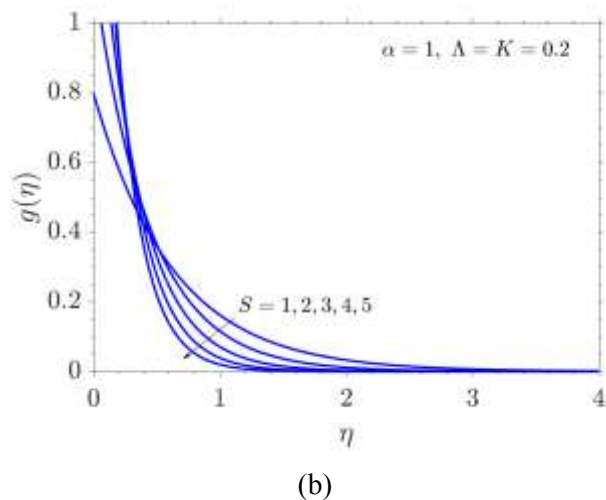
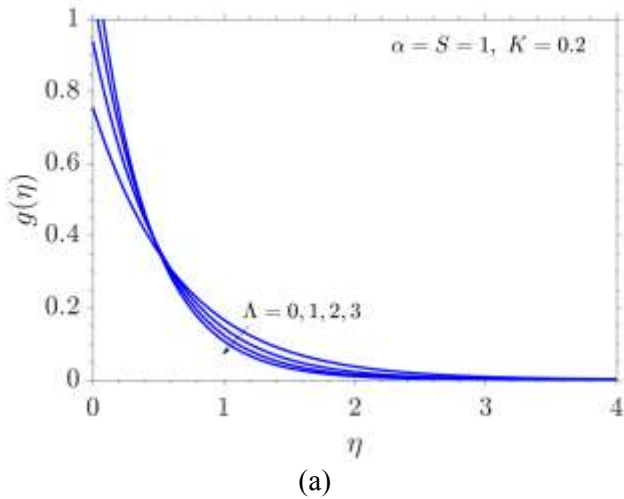


Fig. 5: The angular velocity profiles  $g(\eta)$  on similarity variable  $\eta$  for various values of (a) porous medium parameter  $\Lambda$  and (b) mass transpiration  $S$ .

Figure 6 shows the variation of the skin friction  $Re_x^{1/2}C_{fx}$  with  $\alpha$  for various values of  $S = -0.4, -0.3, -0.2$ , and the fixed parametric values of  $\Lambda = 0.01, K = 1, n = 0.5$ . For a fixed value of  $S$ , the black and red parts of the corresponding graph represent the respective upper and lower branches of the dual solution. For the upper branch of the dual solution,  $Re_x^{1/2}C_{fx}$  increases with an increase in  $\alpha$  for  $-0.03 \leq \alpha \leq 0$ , and  $Re_x^{1/2}C_{fx}$  decreases with  $\alpha$  for  $\alpha > 0$ . On the other hand, in the case of the lower branch of the solution curve,  $Re_x^{1/2}C_{fx}$  is a decreasing function of  $\alpha$  for  $\alpha \leq 0$ , and  $Re_x^{1/2}C_{fx}$  increases with  $\alpha$  for  $\alpha > 0$ . These observations show that the skin friction may decrease or increase depending upon  $\alpha$ .

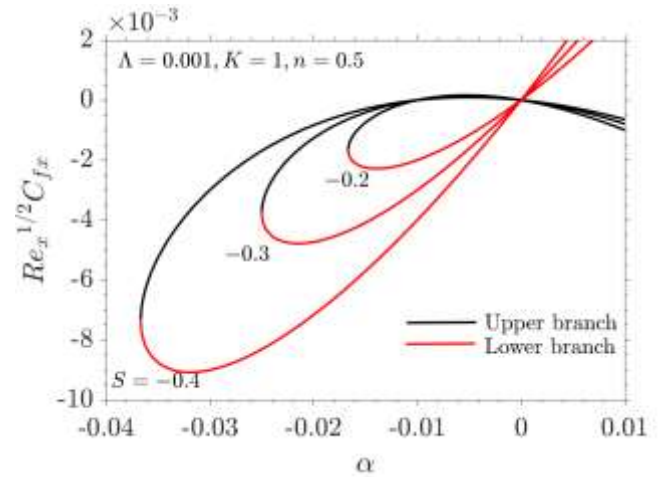
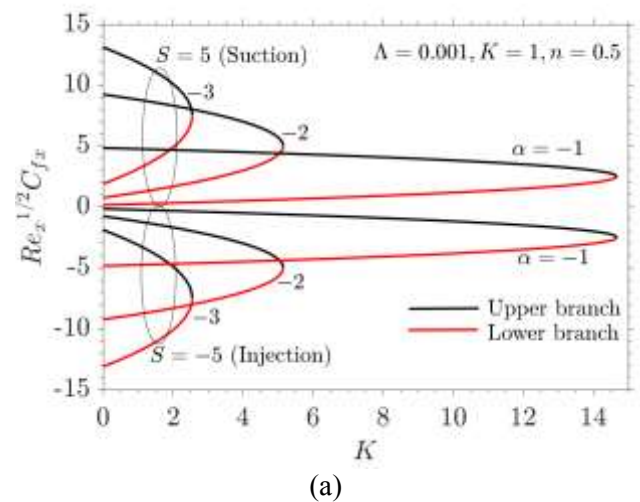
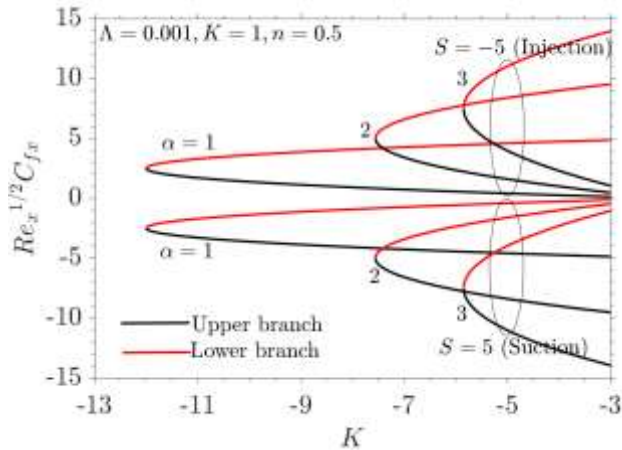


Fig. 6: The effect on  $Re_x^{1/2}C_{fx}$  of  $\alpha$  for various values  $S$ .

Figure 7a and Figure 7b show the variations of the skin friction parameter  $Re_x^{1/2}C_{fx}$  with the microrotation parameter  $K$  for both stretching and shrinking cases, respectively for the fixed parametric values of  $\Lambda = 0.25, n = 0.5$ , and various values of  $\alpha = -3, -2, -1$ . For a fixed value of  $\alpha$ , the black and the red parts of the graph correspond to  $S = 5$  and  $S = -5$ , respectively. Clearly, in the case of stretching, the skin friction  $Re_x^{1/2}C_{fx}$  is greater for suction and smaller for injection but the effect reverses in the case of the shrinking sheet, that is,  $Re_x^{1/2}C_{fx}$  increases with  $K$  for both stretchings as well as shrinking cases.





(b)

Fig. 7: The effect on  $Re_x^{1/2}C_{fx}$  of  $K$  for various values of suction/injection parameter  $\alpha$  for (a) shrinking and (b) stretching cases.

## 6 Conclusion

A micropolar fluid flow with a porous stretching or shrinking sheet in the presence of mass transpiration is investigated analytically and numerically. The highly nonlinear PDEs governing the flow field are transformed into a system of highly nonlinear ODEs by using similarity transformations. The parametric domain for the existence of the unique as well as the dual solutions are investigated. The unique solution is observed at the stretching sheet and dual behavior is observed at the shrinking sheet. Based on the results, the following conclusions can be drawn:

- The solution domain for  $\beta$  increases by increasing the values of the stretching/shrinking parameter  $\alpha$  for the upper branch solution but the effect is reversed in the case of the lower branch, that is, the solution domain for  $\beta$  decreases by increasing the values of the stretching/shrinking parameter  $\alpha$  for lower branch solution as a function of both mass transpiration  $S$  and microrotation parameter  $K$ .
- The solution domain for  $\beta$  is wider for fewer values of microrotation parameter  $K$ .
- Each of the tangential and the angular velocity components is an increasing function of the stretching/shrinking parameter  $\alpha$  and the microrotation parameter  $K$ .
- Each of the tangential and angular velocity components is found to decrease with an increase in the value of the porous medium parameter  $\Lambda$  and the mass transpiration  $S$ .
- The skin friction coefficient increases with an increase in microrotation parameter  $K$ .

## Acknowledgment:

The authors have been supported under project grant no. K\_18-129257 provided by the National Research, Development, and Innovation Fund of Hungary, financed under the K18 funding scheme.

## References:

- [1] T.H. Zhao, M. I. Khan, and Y.M. Chu, Artificial neural networking (ANN) analysis for heat and entropy generation in the flow of non-Newtonian fluid between two rotating disks, *Math. Method Appl. Sci.*, 46, 2021, p.3012-3030. ISSN: 1099-1476, 0170-4214.
- [2] B. C. Sakiadis, Boundary-layer behavior on a continuous solid surface: I. Boundary layer equations for two-dimensional and axisymmetric flow, *A.I.Ch.E. J.*, 7, 1961, p.26-28. ISSN: 0001-1541, 1547-5905.
- [3] B. C. Sakiadis, Boundary-layer behavior on continuous solid surfaces. II. The boundary layer on a continuous flat surface, *A.I.Ch.E. J.*, 7, 1961, p.221-225. ISSN: 0001-1541, 1547-5905.
- [4] L.J. Crane, Flow past a stretching plate, *Z. Angew. Math. Phys.*, 21, 1970, p.645-647. ISSN: 1420-9039, 0044-2275.
- [5] U.S. Mahabaleshwar, G. Lorenzini, Combined effect of heat source/sink and stress work on MHD Newtonian fluid flow over a stretching porous sheet, *Int. J. of Heat and Tech.*, 35, 2017, p.330-335, ISSN: 0392-8764.
- [6] U.S. Mahabaleshwar, P.N. Vinay Kumar, K.R. Nagaraju, G. Bognar, S.N.R. Nayakar, A New Exact Solution for the flow of a fluid through porous media for a variety of boundary conditions, *Fluids*, 4, 2019, p.1-22. ISSN: 2311-5521.
- [7] J. Singh, U.S. Mahabaleshwar, G. Bognar, Mass transpiration in Non-linear MHD flow due to porous stretching sheet, *Scientific Reports*, 9, 2019, 18484. ISSN: 2045-2322.
- [8] M. Turkyilmazoglu, Heat Transfer Enhancement Feature of the Non-Fourier Cattaneo-Christov Heat Flux Model, *Journal of Heat Transfer*, 143(9), 2021, 094501. ISSN: 1528-8943, 0022-1481.
- [9] M. Nazeer, F. Hussain, M.I. Khan, A.ur. Rehman, E.R.R. Zahar, Y.M. Chu, Theoretical study of MHD electro-osmotically flow of third-grade fluid in micro channel, *Appl. Math. Comput.*, 420, 2022, 126868. ISSN: 1873-5649, 0096-3003.



- [10] Y.M. Chu, B.M. Shankaralingappa, B.J. Gireesha, F. Alzahrani, M.I. Khan, S.U. Khan, Combined impact of Cattaneo-Christov double diffusion and radiative heat flux on bio-convective flow of Maxwell liquid configured by a stretched nano-material surface, *Appl. Math. Comput.* 419, 2022, 126883. ISSN: 1873-5649, 0096-3003.
- [11] S. Qayyum, M.I. Khan, T. Hayat, A. Alsaedi, Comparative investigation of five nanoparticles in flow of viscous fluid with Joule heating and slip due to rotating disk, *Physica B Condensed Matter*, 534, 2018, p.173-183, ISSN: 0921-4526.
- [12] M.I. Khan, S. Qayyum, S. Kadry, W.A. Khan, S.Z. Abbas, Irreversibility Analysis and Heat Transport in Squeezing Nanoliquid Flow of Non-Newtonian (Second-Grade) Fluid Between Infinite Plates with Activation Energy, *Arabian J. Sci. Eng.* 45, 2020, p.4939-4947. ISSN: 2191-4281, 2193-567X.
- [13] M.I. Khan, T. Hayat, M. Waqas, A. Alsaedi, Outcome for chemically reactive aspect in flow of tangent hyperbolic material, *J. Mol. Liq.* 230, 2017, 143-151. ISSN: 1873-3166, 0167-7322.
- [14] T. Hayat, S.A. Khan, M.I. Khan, A. Alsaedi, Optimizing the theoretical analysis of entropy generation in flow of second grade nanofluid, *Phys. Scr.* 94, 2019, 085001. ISSN: 0031-8949.
- [15] A.C. Eringen, Simple micro fluids, *Int. J. Eng. Sci.* 2, 1964, p.205-217. ISSN: 0020-7225
- [16] A.C. Eringen, Theory of micro polar fluids, *J. Math. Mech.* 16, 1966, p.118. ISSN: 0095-9057.
- [17] A.C. Eringen, Theory of thermo micro polar fluids, *J. Appl. Math.* 38, 1972, p.480-495. ISSN: 1687-0042.
- [18] K.E. Aslani, U.S. Mahabaleshwar, J. Singh, I.E. Sarries, Combined effect of radiation and inclined MHD flow of a micropolar fluid over a porous stretching/shrinking sheet with mass transpiration, *Int. Jour. Appl. Comput. Math.*, 7, 2021, p.1-21. ISSN: 1641-876X.
- [19] M. Turkyilmazoglu, Flow of a micropolar fluid due to a porous stretching sheet and heat transfer, *Int. J. Non-linear. Mech.*, 83, 2016, p.59-64. ISSN: 0020-7462.
- [20] M. Turkyilmazoglu, Mixed convection flow of magnetohydrodynamic micropolar fluid due to a porous heated/cooled deformable plate: exact solution, *Int. J. Heat and Mass Trans.*, 106, 2017, p.127-134. ISSN: 0017-9310.
- [21] M.M. Rahman, M.A. Samad, M.S. Alam, Heat transfer in a micro polar fluid along a non-linear stretching sheet with a temperature-dependent viscosity and variable surface temperature, *Int. J. Therm. Phys.*, 30, 2009, p.1649-1670. ISSN: 1572-9567, 0195-928X.
- [22] M. Turkyilmazoglu, A note on micropolar fluid flow and heat transfer over a porous shrinking sheet, *Int. J. Heat Mass Transf.*, 72, 2014, p.388-391. ISSN: 0017-9310.
- [23] U.S. Mahabaleshwar, Combined effect of temperature and gravity modulations on the onset of magneto-convection in weak electrically conducting micropolar liquids, *Int. J. Eng. Sci.* 45, 2007, p.525-540. ISSN: 0020-7225.
- [24] G. Bognár, Analytical solutions to the boundary layer problem over a stretching wall, *Computer and Mathematics with Applications*, 61(8), 2011, p.2256-2261. ISSN: 0898-1221.
- [25] G. Bognár, M. Klazly, K. Hriczó, Nanofluid flow past a stretching plate, *Processes* 8(7), 2020, p.827. ISSN: 2227-9717.
- [26] G. Bognár, K. Hriczó, Series solutions for Marangoni convection on a vertical surface, *Mathematical Problems in Engineering*, 2012, Article ID 314989. ISSN: 1024-123X, 1563-5147.
- [27] Z.H. Khan, M. Qasim, I. Neema, W.A. Khan, Dual Solutions of MHD boundary Layer Flow of a Micropolar fluid with weak concentration over a stretching/shrinking sheet, *Commun. Theor. Phys.* 67, 2017, p.449-457. ISSN: 0253-6102.
- [28] T.C. Chaim, Magneto hydrodynamic heat transfer over a non-isothermal stretching sheet, *Acta Mechanica*, 122, 1997, p.169-179. ISSN: 1619-6937, 0001-5970.

### **Contribution of Individual Authors to the Creation of a Scientific Article (Ghostwriting Policy)**

-Rishu Garg carried out the formal analysis and simulation.

-Jitender Singh has written the original draft.

-U.S. Mahabaleshwar and Okjunjon Sayfidinov have been participated in the writing and review of the paper.

-Gabriella Bognár has participated in the writing and the review of the paper and in the organization of funding.

### **Sources of Funding for Research Presented in a Scientific Article or Scientific Article Itself**

The authors have been supported under project grant no. K\_18-129257 provided by the National Research, Development, and Innovation Fund of Hungary, financed under the K18 funding scheme.

### **Conflict of Interest**

The authors have no conflict of interest to declare.

### **Creative Commons Attribution License 4.0 (Attribution 4.0 International, CC BY 4.0)**

This article is published under the terms of the Creative Commons Attribution License 4.0

[https://creativecommons.org/licenses/by/4.0/deed.en\\_US](https://creativecommons.org/licenses/by/4.0/deed.en_US)